Pergamon

Int. J. Solids Structures Vol. 35, No. 19, pp. 2505–2521, 1998

0020–7683/98 $19.00 + .00

PII: S0020–7683(97)00147–9

FRACTURE STATISTICS MODELING OF LAMINATE COMPOSITES

CONSTANTIN BAXEVANAKIS
Centre des Matériaux P.M. Fourt, Ecole des Mines de Paris, BP 87, F91003 Evry Cedex, France

DOMINIQUE JEULIN
Centre de Morphologie Mathématique, Ecole des Mines de Paris, 35 rue de Saint-Honoré, F77305 Fontainebleau, France

BÉACHLÉ LEBON and JACQUES RENARD
Centre des Matériaux P.M. Fourt, Ecole des Mines de Paris, BP 87, F91003 Evry Cedex, France

(*Received* 19 *May* 1997)

Abstract—A general approach to predict the behavior of the failure stress of fibre composites is proposed. Based on a probabilistic micro–macro approach, it accounts for the statistical distribution of defects along the fibres and on transverse specimens. After the introduction of a statistical volume element containing at least one critical defect, a finite element analysis is used to simulate the progression of damage in laminate specimens. The scale effects and the influence of the involved parameters on the failure of the material were studied for the following conditions: fiber breaks, transverse fracture, fracture of composite materials ($[0, 90]_s$ and angle ply laminates). © 1998 Elsevier Science Ltd. All rights reserved.

1. INTRODUCTION

The use of organic matrix/high modulus fiber composites is increasing in space and aeronautic fields. Carbon fiber reinforced composites are used in many applications where safety requirements play an important part in the design process. The composites are made of sequences of layers of long fibers embedded in a matrix. These materials have brittle characteristics and they show a large variability of fracture properties. Their strong heterogeneity and their anisotropy imply special kinds of damage processes, which require the development of new approaches and models to predict their behavior under various loading conditions. The main problem for the designer is the estimation of the scale effect, namely how the size influences the scatter of the material properties, based on experimental tests and on their extension up to full scale. In this study, a method is proposed for estimating the fracture stress statistics of a composite material under the following loading conditions: parallel to the fibers of a unidirectional layer; transverse to the fibers; and finally applied to laminate composites under off axis solicitations. This method is based on a micro–macro approach using appropriate statistics and finite elements at different scales. The statistical information concerning the distribution of defects at the micro scale is obtained through experiments. The above method is applied to the fracture of T300/914 carbon fiber reinforced composites.

2. METHODOLOGY

In the case of materials where a diffuse damage grows before fracture, an efficient method to predict the probability of fracture is based on numerical simulation techniques combining finite element calculations of the stress and strain fields, and Monte-Carlo simulations for the local fracture criterion. We developed a specific approach (Baxevanakis, 1993a, 1993b, 1994, 1995; Jeulin, 1995), that can be applied to various types of fracture of composite materials, as illustrated in this paper. It is based on the following steps:

(i) identification of the population of defects contained in the material by means of specific mechanical tests and/or macro–micro calculations;
(ii) determination of a statistical mesh and of a statistical volume element (SVE) depending on a local fracture criterion;
(iii) introduction of statistical information and of the fracture criterion in a finite element calculation;
(iv) study of the fracture behavior on a first scale, namely on elementary representative volume element (RVE);
(v) if necessary, the material may be considered as a set of RVE studied on a larger scale.

The introduction in finite element calculations of a characteristic scale in the material by the SVE, namely the minimal volume containing at least one defect that can be broken during the applied loading, is a crucial point in the model. Indeed, without any SVE, unwanted mesh effects occur for the overall fracture stress in the simulations, as explained below in Section 3. The SVE itself has to be determined from specific mechanical tests, as illustrated in further sections, and depends on the type of fracture (fiber fracture, transverse fracture).

3. FIBER FRACTURE

The first step of this study concerns the fracture from a solicitation along the fibers. Experimental tests of a carbon epoxy T300/914 were made on specimens with a 60% fiber volume fraction and with two different gage lengths 100 and 200 mm (Baxevanakis, 1993a, 1993b, 1994, 1995). From the fracture statistics estimated with these specimens, no significant scale effect was apparent.

3.1. *Identification of the statistics of defects on fibers*

The statistical distribution of defects on fibers is estimated using specimens made of a single fiber embedded in the resin, and a multi-fragmentation test (Baxevanakis, 1993a). The cumulative density $\theta(\sigma)$ of defects along a carbon fiber (i.e. the average number of defects per unit length with fracture stress lower than σ) as a function of the applied stress σ was modelled by a sigmoidal function:

$$\theta(\sigma) = A\left(1-\exp-\left(\frac{\sigma-\sigma_s}{\sigma_0}\right)^m\right) \tag{1}$$

where A is the maximum number of defects per unit length (8.66 mm^{-1}), σ_0 is a scale parameter (6318), σ_s is a threshold stress (equal to zero in the present case), and m a shape parameter (estimated to 7.26 in the present case). This function can be approximated for the weak values of the stress by a power law function $\theta(\sigma) = A(\sigma-\sigma_s/\sigma_0)^m$, as used in the case of the Weibull distribution which fits well results of single fiber tests. Assuming that a fiber with length L breaks under a homogeneous tensile stress σ with the weakest link assumption, the probability distribution of the fracture stress σ_R of the fiber is obtained (Jeulin, 1991):

$$P\{\sigma_R < \sigma\} = 1-\exp(L\theta(\sigma)). \tag{2}$$

Equation (2) is valid for point defects distributed according to a Poisson point process. According to our data, the sigmoidal distribution function is valid for a fiber length $L \geqslant 0.5$ mm, corresponding to the average fragment length at the saturation limit of the single fiber specimen.

3.2. *Introduction of a statistical volume element (SVE)*

To simulate the progress of damage in a material containing defects, we must be able to decide when and how we have to break parts of a loaded specimen. For this purpose, a

coupling between fracture statistics and finite elements was developed. It is based on the digitization of the continuous medium, which is represented by a mesh with a number of finite elements (f.e.). Assuming that each f.e. represents a defect with an associated fracture stress σ_R, the distribution of the fracture stress depends on the size of the f.e. When it decreases, the convergence of the stress and strain field occurs, while the probability of fracture given by eqn (2), based on the weakest link assumption applied to the f.e. tends to zero for any applied stress σ. As a result, refining the finite element mesh would result in an increase of the fracture stress to infinity. Consequently we consider a statistical mesh (statistical volume element SVE), where each element contains at least one defect (with a length $L_s \geqslant 0.5$ mm in the present case) superimposed on the finite elements mesh, as illustrated on Fig. 1 for a representative volume element RVE containing 12 fibers; the different gray levels represent the values of the random fracture stress σ_R of the defects (and consequently of the SVE) along the fibers, where the length of a f.e. is 0.1 mm to warrant the convergence of stress and strain fields. The SVE introduces a length scale which is a material property and has to be determined from experiments: it will depend on the type of epoxy and fibers and on their adhesion. In the present case, its size, and the corresponding fracture stress, was estimated from multifragmentation tests made on single fibers, as

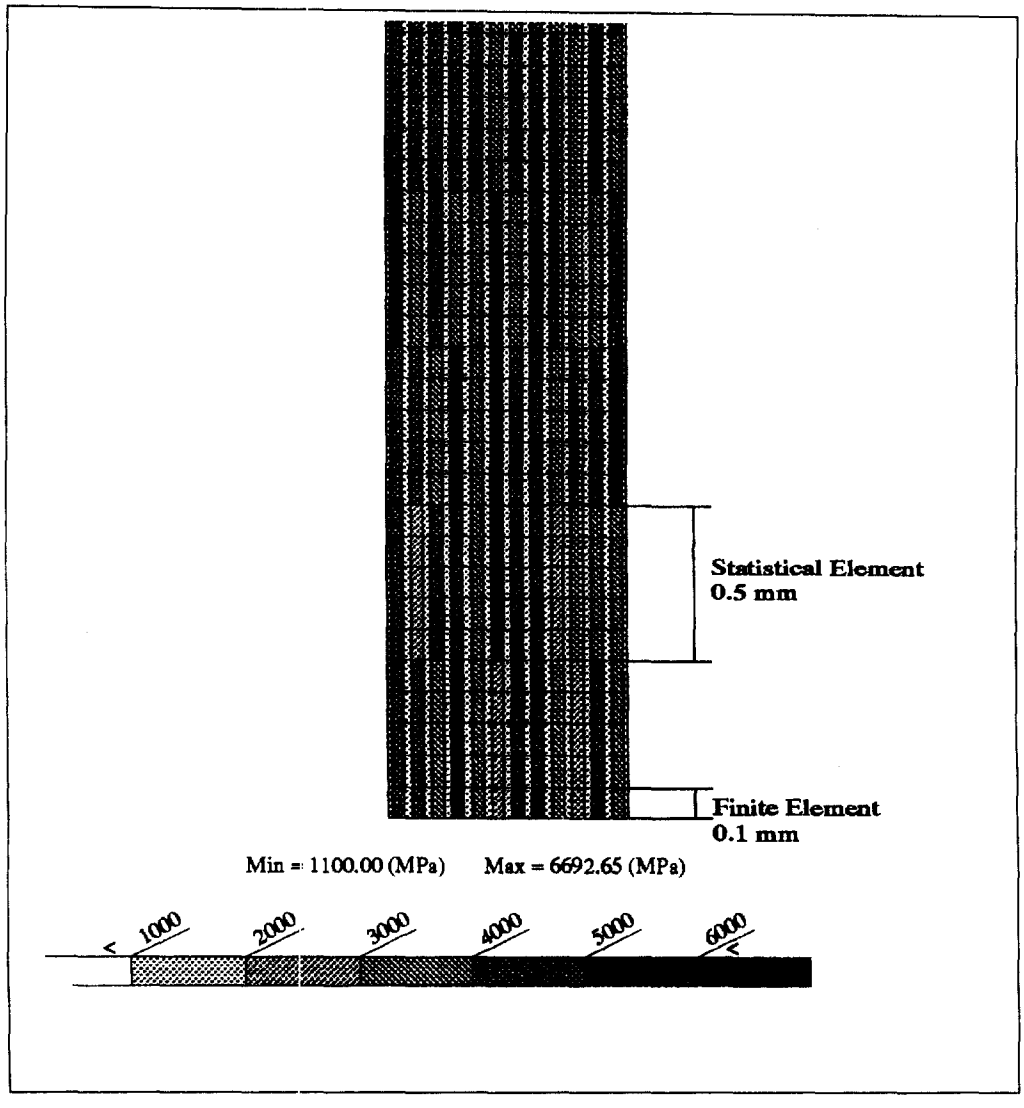

Fig. 1. Simulation of a distribution of the fracture stresses in the RVE.

detailed in (Baxevanakis, 1993a). Its fracture stress is a random variable following the distribution function (2) when the applied stress field is homogeneous; in other cases, we can compare the fracture stress σ_R of the SVE with the average applied stress $\bar{\sigma}$; a more rigorous fracture criterion of the SVE is derived from the weakest link assumption and the Poisson point process:

$$P\{\text{fracture of the SVE}\} = 1-\exp\left(\int_{\text{SVE}} \theta(\sigma(x))\,dx\right) = 1-\exp(V\theta(\sigma_{eq})) \tag{3}$$

where V is the volume (here the length L_s) of the SVE, and σ_{eq} an equivalent stress giving the same formula as for the homogeneous stress field over the SVE. By application of eqn (3), it is easy to provide Monte-Carlo simulations of the random fracture stress of the SVE, even when it is located in large stress gradients: the SVE will be broken when the applied σ_{eq} is larger than the random fracture stress obtained by simulation of a random variable following the distribution given by eqn (2).

3.3. *Fracture statistics from two-dimensional simulations of composites*

In calculations, a plane stress state is assumed; the element type used was four-node with a linear shape function and four-Gauss integration points [with the ZEBULON f.e. code (Burlet, 1986)]. When the average stress calculated at the Gauss point of a f.e. overcomes the associated fracture stress σ_R, the f.e. is broken (its stiffness is replaced by the matrix stiffness, the Young's modulus of the matrix being a 100 times lower than the modulus of the fiber); a damaged length L_d, where the drop of the stiffness occurs, is introduced ($L_d = 0.1$ mm in the present case); it is interpreted as a parameter of the interfacial bound between fiber and matrix. Uniform strains are applied on the boundary of the RVE. Thirty realizations of the RVE with periodically distributed fibers (between 3 and 12) and a length varying between 1 and 15 mm were simulated. The mechanical behavior of a simulation obtained by homogenization is illustrated in Fig. 2. It is in good agreement with the experiments.

The same procedure, based on 30 simulations per case, is adopted to describe the fracture behavior of the material on the next scale (meso scale). In this case a SVE represents a previous RVE (having eight fibers, 12 mm length, $V_f = 60\%$) with the obtained fracture statistics, and the f.e. which belong to a same SVE have the same fracture stress σ_{Re}. The influence of the volume fraction variability on the fracture behavior of the composite was studied from further simulations reproducing the statistical distribution of V_f obtained by image analysis, as reported in details elsewhere (Baxevanakis, 1994; Baxevanakis, 1995).

We report now the results of the simulations concerning the fracture statistics deduced from simulations.

From RVE simulations, the scale effect on the average strength and on the critical density of defects at fracture is illustrated in Fig. 3: for a RVE containing more than six fibers and with length longer than 8 mm, the cumulative fracture distribution obtained by simulations is seen to tend towards on asymptotic distribution [as shown from a statistical model in Smith (1981)]. The same observation is made concerning the critical density of defects. From the record of the coordinates of fiber breaks during the simulations, a uniform distribution of damage over the RVE was observed at the same critical size. The evolution of the sampled defects during the progress of damage can be summarized as follows: first a diffuse damage samples the weakest defects on fibers. Other defects of the whole population are broken, due to the stress concentration in the vicinity of the already broken elements. After the failure of a number of fibers (seven or eight in the present case), a crack orthogonal to the load axis is formed, the stress concentration factor being too large for any fiber to stop the propagation, as already shown by analytical models with simplified assumptions (Hedgepeth, 1961; Batdorf, 1982; Bader, 1982). At this intermediate scale, a scale effect is observed for RVE of small length only, while later an asymptotic distribution is obtained, resulting from the effect of a critical density of the defects causing the fracture [a statistical proof of this type of fracture behavior is given in Jeulin (1991)]. This distribution,

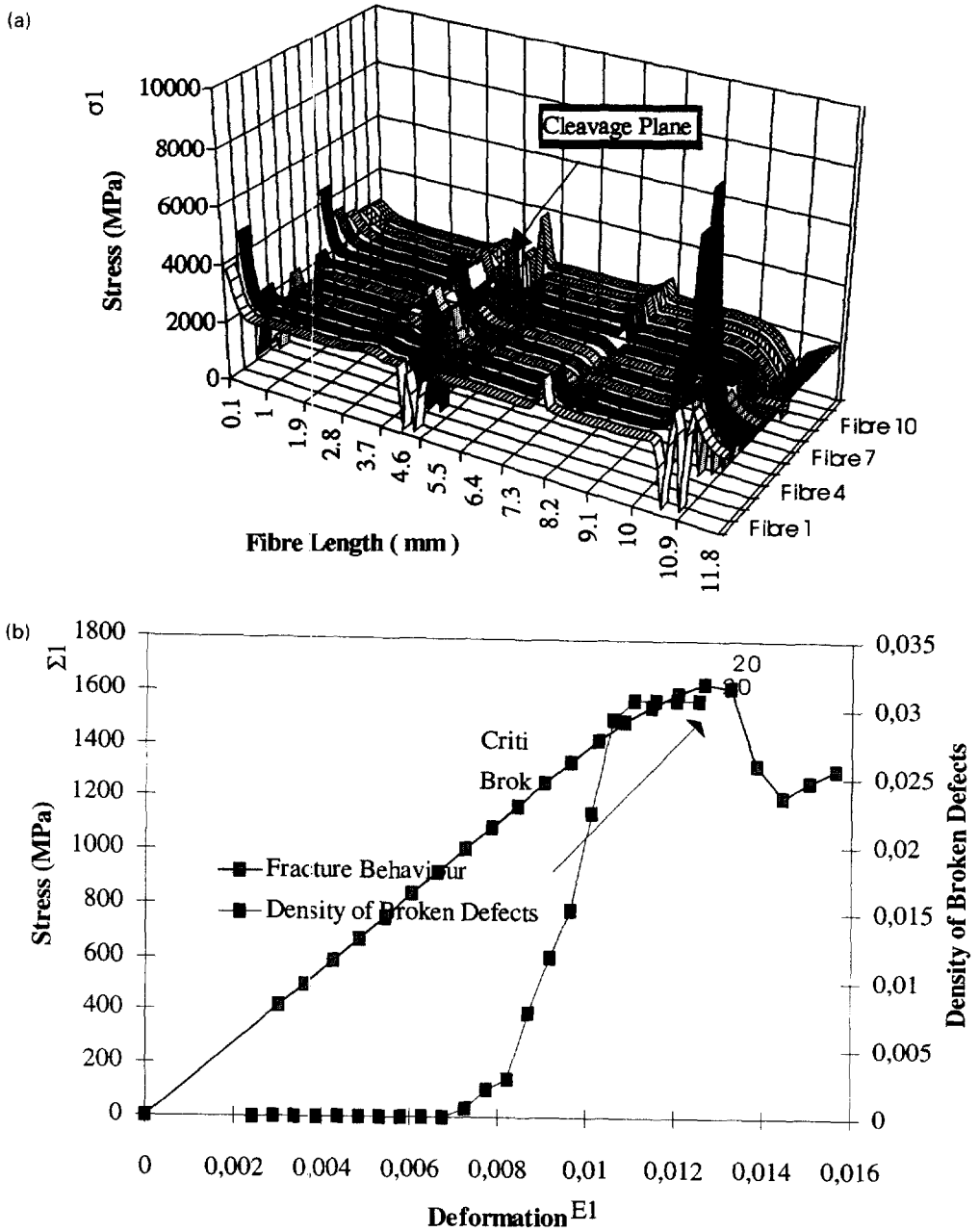

Fig. 2. (a) Stress field along the fibers in a simulation at the increment no. 20; (b) fracture behavior of a representative volume element (same domain as for Fig. 2(a)), obtained by homogenization.

deduced from simulations, compares well with the experimental distribution (Fig. 4); tests were made on specimens with a 10×1 mm^2 cross-section and with two different gauge lengths (100 and 200 mm), cut from 300×300 mm^2 plates. Tests were performed with an Instron testing machine, using a 0.1 mm min^{-1} crosshead speed and acoustic emission to detect the damage threshold in the specimen.

Additional calculations were made at a meso scale, the composite being now an assembly of SVE made of previous RVE. No important size effect is observed and over a certain size the fracture behavior of the material becomes completely deterministic; the estimated fracture stress is lower than on the previous scale and than in experiments, the fracture being caused by the failure of the most critical defects. For a random V_f, the average fracture stress is again lower and its dispersion is higher, because the fracture is

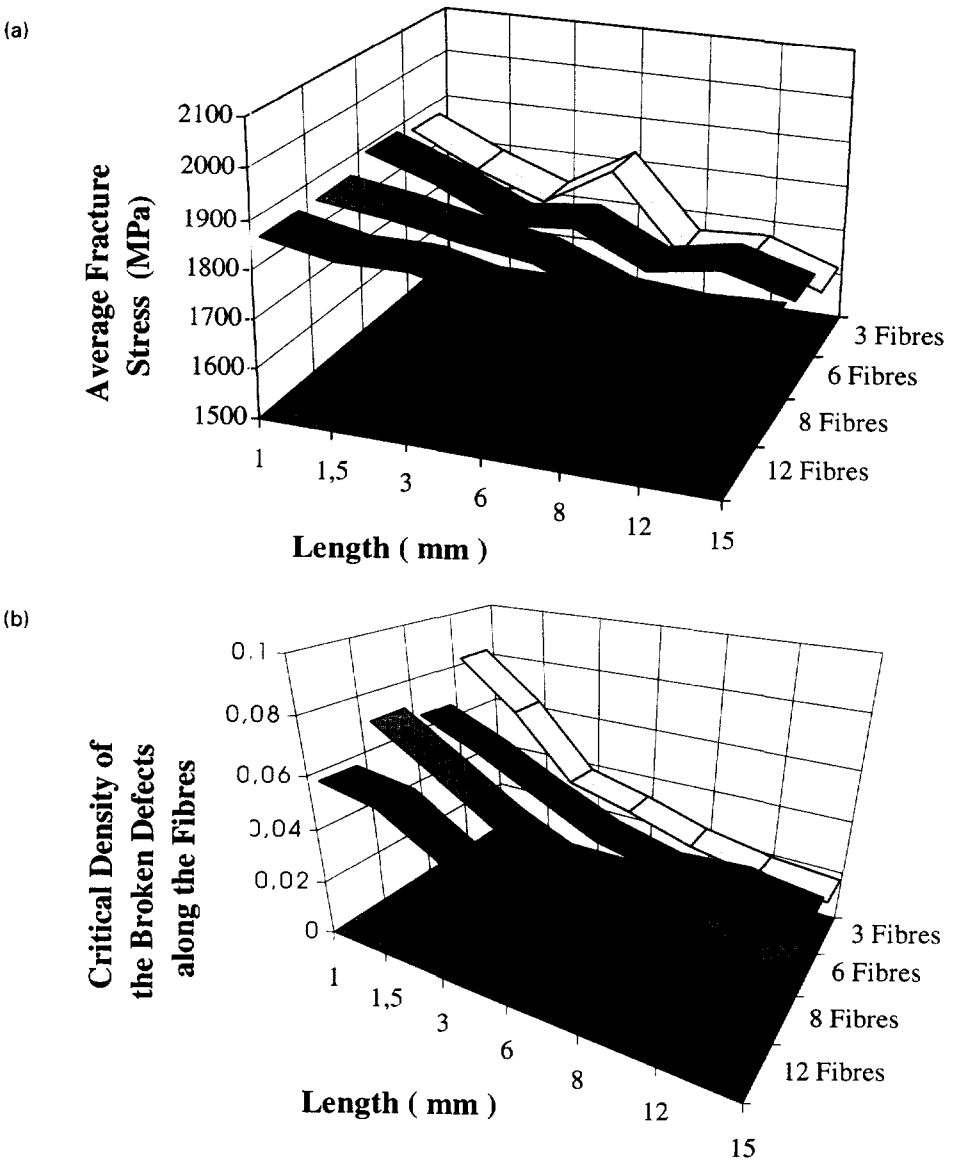

Fig. 3. (a) Average fracture stress as a function of the size of the element (30 simulations were carried out for each size); (b) average value of the critical density of broken defects, calculated at the fracture of the RVE, as a function of the size of the element (30 simulations for each size).

induced by the RVE of low fiber volume fractions. The discrepancy with experiments results from the use, in the model, of the RVE stiffness dropping to zero after the break, causing the fracture of the whole composite. In fact a progressive fracture behavior based on continuum damage mechanics could be adopted.

4. TRANSVERSE FRACTURE OF A LAYER

The experimental study and the model are now developed on a meso-scale, where data are available at a mesoscale; fracture tests were made on composites with two thicknesses of the 90° solicited layer (0.25 and 0.5 mm).

4.1. *Identification of the population of defects*

According to experimental observations, the transverse cracking in 90° plies is the most important damage process (Reifsnider, 1982; Wang, 1984). It appears early during

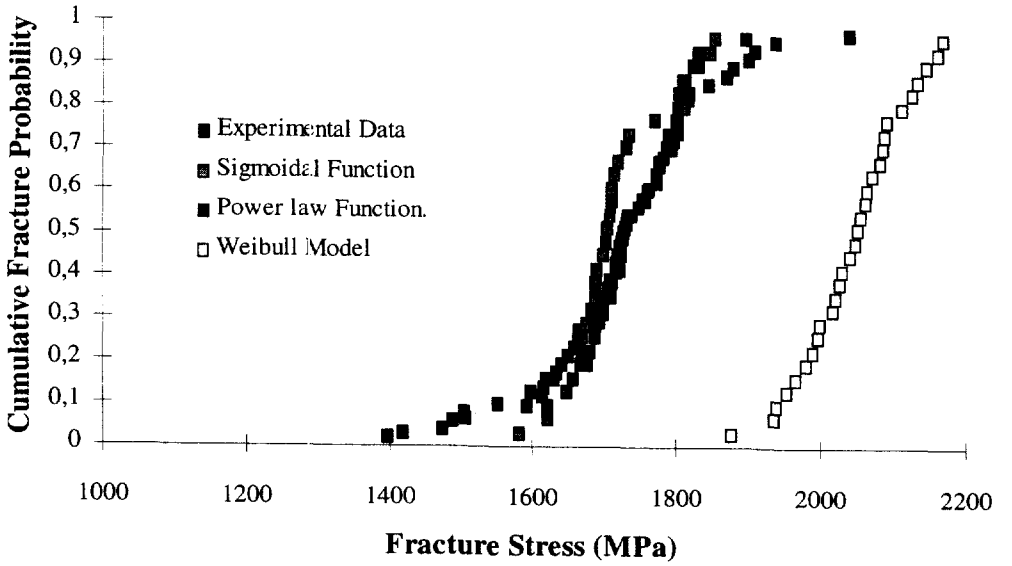

Fig. 4. Cumulative fracture distribution of the characteristic RVE (eight fibers with length 12 mm), as a function of the tested density functions of defects along the fibers: comparison with the experimental data.

the loading, and it grows until a saturation state characterized by an inter crack distance (1 crack : mm). Then the distance between two cracks is too small to allow the loading of the matrix and the apparition of new cracks.

Multicracking tests of a cross-ply ($[0_{n_1}, 90_{n_2}]_s (n_1, n_2 = 1, 2)$) composite (generalizing the multi-fragmentation test of a single fiber) provide information on the density of cracks in the ply at 90° as a function of the macroscopic stress. A unidirectional tensile test at room temperature is chosen to study the damage inside the middle plies. Observation of the growth of the damage is possible using a optical microscope on a polished area of the specimen, and counting the number of cracks.

The resulting density of cracks can be converted into an estimation of the defect density $\theta(\sigma)$ by a macro–micro calculation. Using finite element calculation and a homogenization procedure, the local stress σ at crack initiation is estimated, and therefore the crack density is converted into an experimental cumulative density of defects $\theta(\sigma)$.

4.1.1. *Method of calculation of the local fracture stress.* The chosen fracture criterion is local and, therefore, it is necessary in a first step to calculate the stress field within a cracked ply. A cell representing the damaged material is chosen (Fig. 5) and meshed with hexaedral elements with a quadratic interpolation. Cracks are in the end of the cell and the entire specimen can be obtained by periodicity.

In order to identify the population of defects from experimental measurements in a layered composite, we used the following method: to any value of the crack density D_i is attributed a corresponding macroscopic stress Σ from the $(D_i$–$\Sigma)$ experimental curve, and

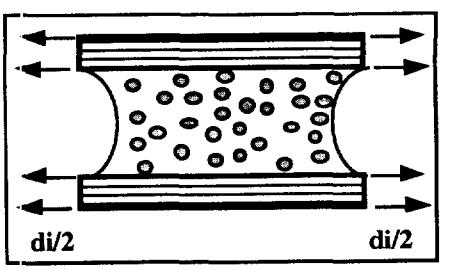

Fig. 5. Cracked cell for the calculation of the local fracture stress in transverse fracture.

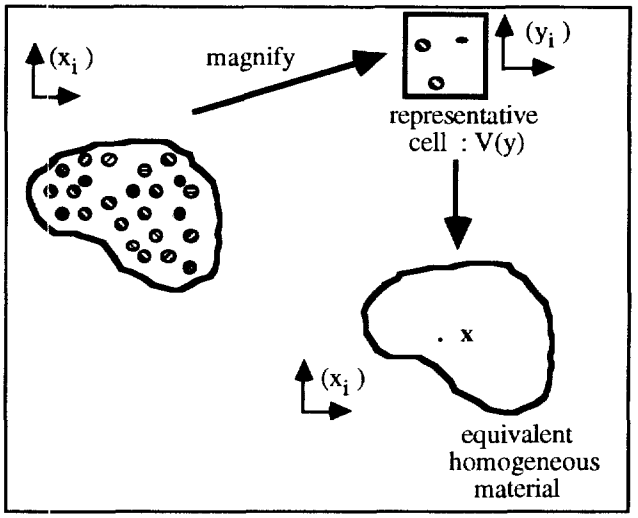

Fig. 6. The averaging method, different scales.

a value of the strain E_i from the (Σ–E) curve; the value of the parameter d_i defined in Fig. 5, to use for the unit cell is calculated and applied to the cell; finally, one solves the final f.e. problem corresponding to Fig. 5.

Before introducing the different fracture criteria, we will describe the homogenization technique used in the numerical calculation. A macro–micro approach enables us to model the behavior of the damaged and undamaged material. The structure is supposed to be periodic by zone. An equivalent homogeneous material without any cracks is substituted for the cracked material. Cracks are taken into account through the "effective stress" concept and the derived equivalent moduli, obtained by homogenization, as described in the Appendix.

4.1.2. *The local fracture criterion.* As shown on Fig. 7, a crack propagates under mode I, induced by a stress $\sigma_{11}(x)$ normal to the crack direction. The corresponding inter crack distance is given by

$$L_{sat} = 2L_c. \tag{4}$$

In this model, the material is a continuous chain of statistical volume elements (SVE)

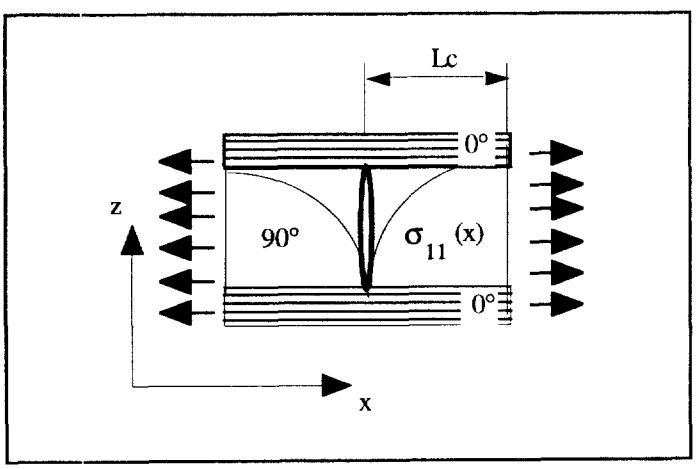

Fig. 7. Definition of the SVE (statistical volume element) for transverse fracture.

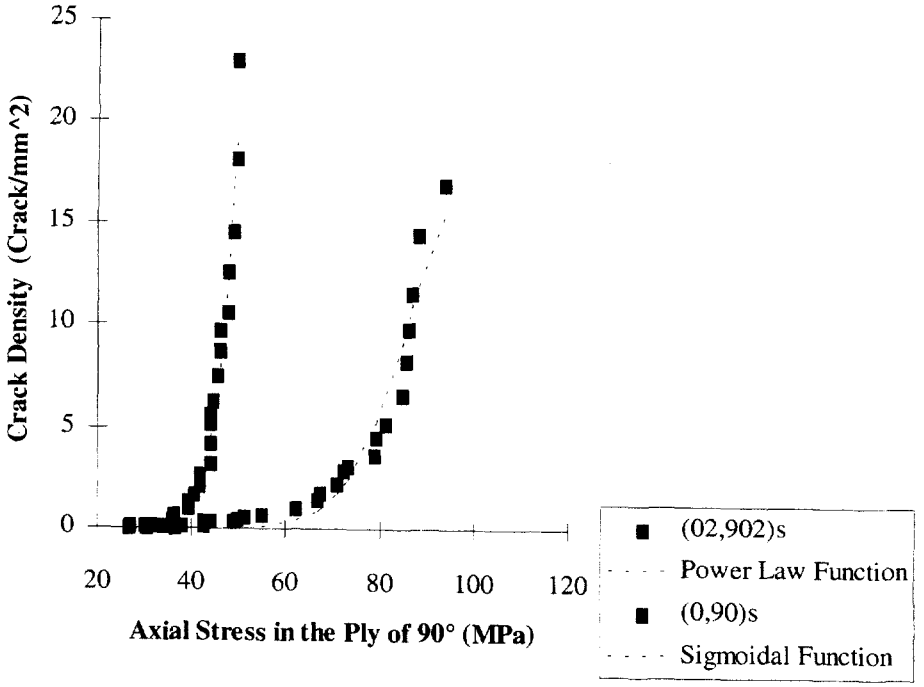

Fig. 8. Crack density (crack/mm^2) as a function of the axial stress in the ply of 90° for the two studied laminates $[0, 90]_s$ $[0_2, 90]_s$.

with a length equal to L_{sat}. Consequently, it corresponds to the minimal volume for a crack to appear in 90° plies.

As said before, the main idea of our approach to simulate the fracture behavior, is to apply a weakest link hypothesis to each SVE. In the present case, when the local rupture criterion is reached in a SVE, the material is weakened. Its initial rigidity is replaced by a damaged one. Let us remind that with the weakest link hypothesis, the fracture probability of a SVE is given by the eqn (2) where $\theta(\sigma)$ is the cumulative broken defect density according to the stress $\sigma = \sigma_{11}(x)$ considered constant in the SVE.

From the previous remark, we can propose an estimator of the defect density: considering a length L_f of material with cracked cells, one could use the estimation $\theta(\sigma) = 1/L_f$. However, since a constant stress is required in the SVE, $\theta(\sigma)$ is estimated by:

$$\theta(\sigma) = \frac{1}{(L_f - 2L_c)e} \tag{5}$$

where $L_f = 1/D_i$, D_i being a given crack density and e the thickness of the cracked plies.

From Fig. 8, it appears that the estimated $\theta(\sigma)$ depends on the thickness, and therefore cannot be considered an intrinsic property of the material since it combines crack initiation and propagation. However, we use in simulations the curve obtained for the corresponding thickness; the population of defects of the smaller thickness is modelled by a sigmoidal function [eqn (1)] with $A = 17.04\ \text{mm}^{-2}$, $\sigma_0 = 86.7$ and $m = 11.04$; for the larger thickness, the density $\theta(\sigma)$ is modeled by a power law function (as in the Weibull distribution) with $\sigma_0 = 38.6$ and $m = 11.91$. In a similar study, the considered defects are microcracks with a Weibull size distribution, which are introduced in simulations based on linear fracture mechanics concepts (Wang, 1984).

4.2. *Definition of a statistical volume element*

The same approach as for the fiber break is used for simulating the transverse multicracking: now a SVE_{90} containing a single critical defect for crack initiation is defined from the average crack spacing at saturation (Fig. 7). The length of the SVE_{90} is 0.835 and

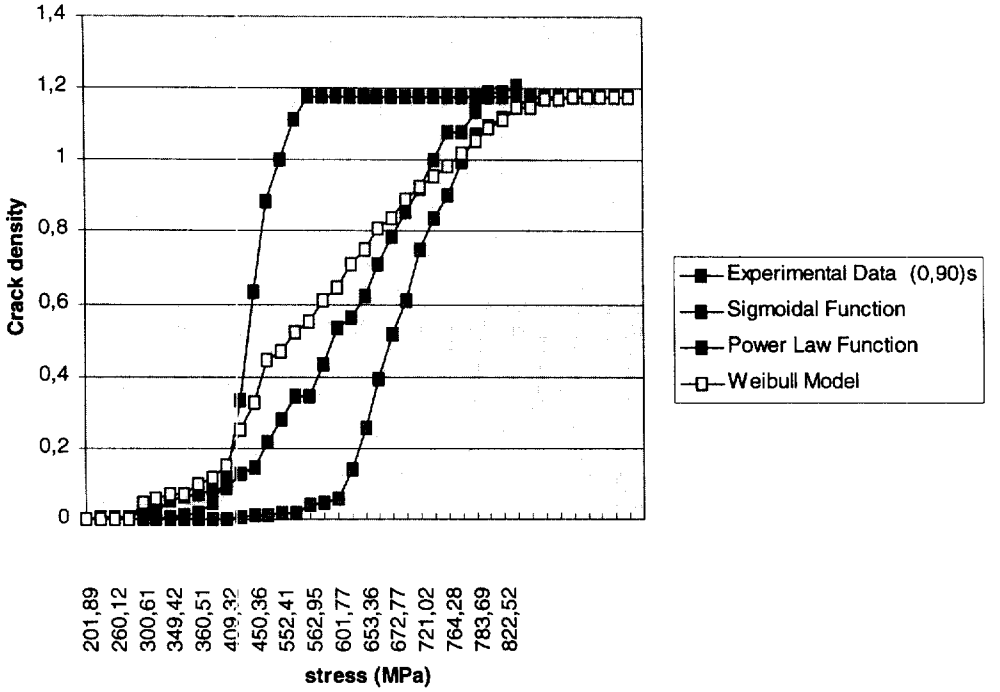

Fig. 9. Comparison between the experimental and the numerical prediction of the evolution of the crack density as a function of the applied stress.

0.96 mm for the 0.25 and 0.5 mm thickness, and its width is the thickness of the layer. To every SVE_{90} is attributed a random fracture initiation stress obeying eqn (2) where L is replaced by the volume V_{SVE} of the SVE. An f.e. mesh is superimposed on specimens with length 100 mm.

4.3. *Multicracking simulation*

For the calculations, the 0° layer is assumed to be orthotropic linear elastic, while the 90° layer f.e. is damaged when reaching its fracture initiation stress (the damaged elastic stiffness is replaced by the equivalent stiffness of the cracked material). A mesh with 2880 rectangular f.e. (using the same element as in Section 3.3) for the 0.5 mm and with 3800 f.e. for the 1 mm thickness was used in simulations (30 realizations per thickness). The kinetics of the damage process is very well reproduced (Fig. 9) for the 0.5 mm thickness. The agreement is limited to the lower crack initiation stresses for the other thickness because the crack propagation and the interaction between cracks are neglected in the model.

5. TRANSVERSE FRACTURE OF A LAMINATE COMPOSITE

5.1. *Geometry of the simulations*

The two previous approaches are combined for the simulation of the fracture of laminate composites $[0_{n_1}, 90_{n_2}]_s$ with two thicknesses (0.5 and 1 mm), under a tensile stress parallel to the fibers of the 0° layer. The multicracking process is initiated in the 90° layer. For the simulation of 30 samples per case, the same SVE_{90} as for the transverse cracking (with the corresponding fracture statistics) is used in the 90° layer. A mesh made of 50 SVE is used for these simulations. For the 0° layer, two extreme situations were investigated (Fig. 10): (i) to a SVE_0 having the same length as the SVE_{90} and with the thickness of the layer, is affected a random fracture stress generated according to the asymptotic 0° distribution: (ii) a uniform random fracture stress is attributed to every 0° layer, assuming the absence of scale effect. In both cases is studied the statistical distribution of the fracture stress of the composite and of the crack density at saturation in the 90° layer. To simulate the loading until fracture (1.3% strain), 40 steps of calculation are implemented in the

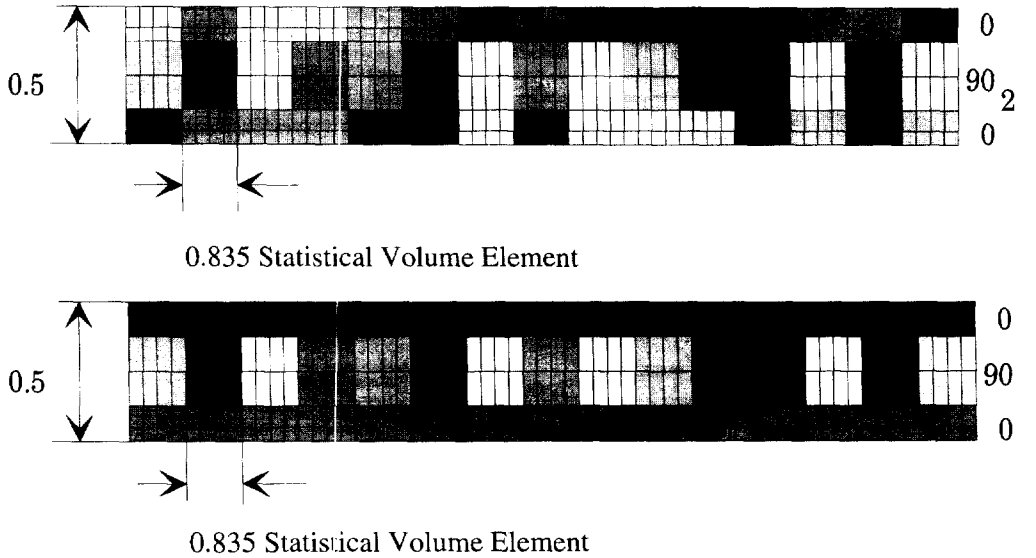

Fig. 10. (a) Coupling between failure statistics and finite element: to each $SVE0_0$ of the ply of 0° is associated a random stress following the asymptotic 0° distribution; (b) Coupling between fracture statistics and finite element: assuming no scale effect in the fracture of the 0° layer, a uniform random fracture stress is attributed to every 0° ply.

nonlinear part of the ZEBULON f.e. code, using a tridimensional mesh. The previous calculations were done using a pseudo three-dimensional approach and bidimensional finite elements. In this case a full tridimensional approach is adopted in order to obtain more precise results. Tridimensional finite elements with eight nodes and quadratic interpolation were used; three meshes were investigated, a coarse one, with 160 finite elements, and two refined meshes with 1000 and 2550 finite elements.

5.2. *Transverse fracture statistics of a laminate*

The results of the simulations obtained for the case of a $[0_2, 90_2]_s$ composite show that the first assumption (i) given in Section 5.1 produces a deterministic behavior of the fracture stress, while the second case (ii) reproduces correctly the mean value (892 MPa), the standard deviation (34.4 MPa) of the fracture stress observed on experiments (869 and 30.6 MPa). A series of 30 tensile tests were performed on $[0_2, 90_2]_s$ specimens, the study of the fracture stress being detailed is described in [Lebon, 1995]. This is illustrated by Fig. 11

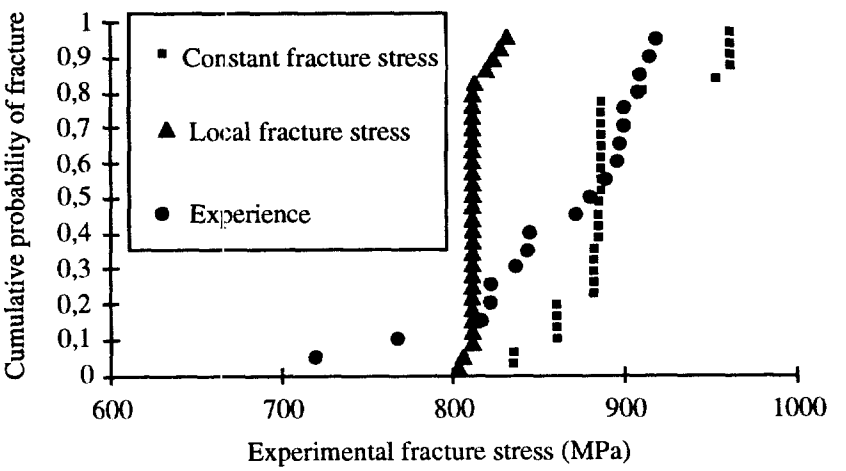

Fig. 11. Comparison between the predicted and the experimental transverse fracture stress distributions.

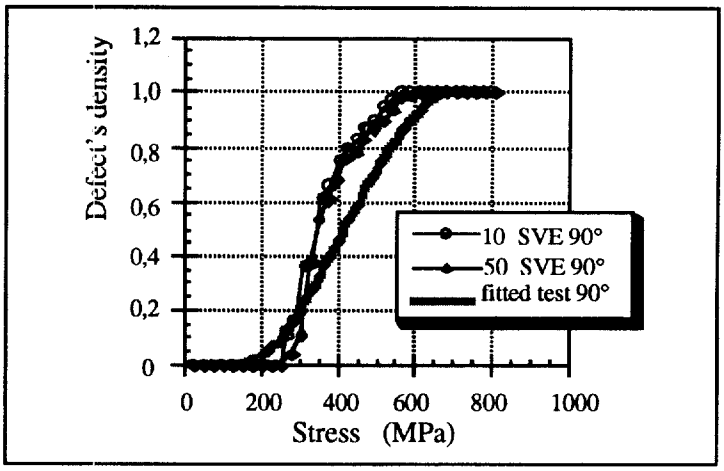

Fig. 12. Prediction of the damage kinetics for the transverse fracture of a laminate composite.

showing a comparison between the experimental and simulated distributions of the fracture stress. This result is in agreement with the absence of scale effect observed in the fiber fracture study, and should be useful for further simulations of composites at different scales.

5.3. *Prediction of the damage kinetics*

As in Section 4.3, we can study the evolution of the crack density when increasing the applied stress during the simulation. This is shown in Fig. 12 obtained for a $[0_2, 90_2]_s$ composite. It appears that the simulated kinetics is slightly more pessimistic than the actual one, since the growth of the crack density is a bit faster. In this simulation, there is no incidence of the number of SVE (10 and 50 SVE) on the kinetics; this means that no apparent size effect is seen for this type of solicitation.

6. OFF AXIS FRACTURE OF LAMINATE COMPOSITES

In this section, a generalization of the previous models to the off axis fracture is proposed. An additional fracture criterion leads to simulations of the complete fracture behavior of angle ply laminate under tensile loading. In the absence of reliable experimental data for this kind of solicitation, we used for comparison results of simulations, obtained with a software based on a micro–macro continuous approach, developed in (Renard, 1993a). Starting from experimental curves of the stress–strain obtained for each laminate, this program provides the evolution of crack densities. The following sequences of stacking of composites are studied: $[0_2, \alpha_2]_s$ with $\alpha = 45$, 60 and 80°.

6.1. *Calculation of the mean stress field of the middle ply*

Using the same features as for the flat laminate $[0_2, 90_2]_s$, one calculates the mean stress field of the middle plies of the angle ply laminate. According to the numerical results, the stress field is complex and very heterogeneous, therefore, in order to impose a constant stress in a SVE, a corrected density is used, accounting for the volume under the higher solicitation. In order to correct the density, the area in the middle ply where the average stress is constant is considered (its length is equal to L) and the length L_c (defined in Fig. 7) is replaced by L. So doing, we took into account the corrected density due to stress variation in the calculated cell. A more rigorous approach would use the formulation given by eqn (3).

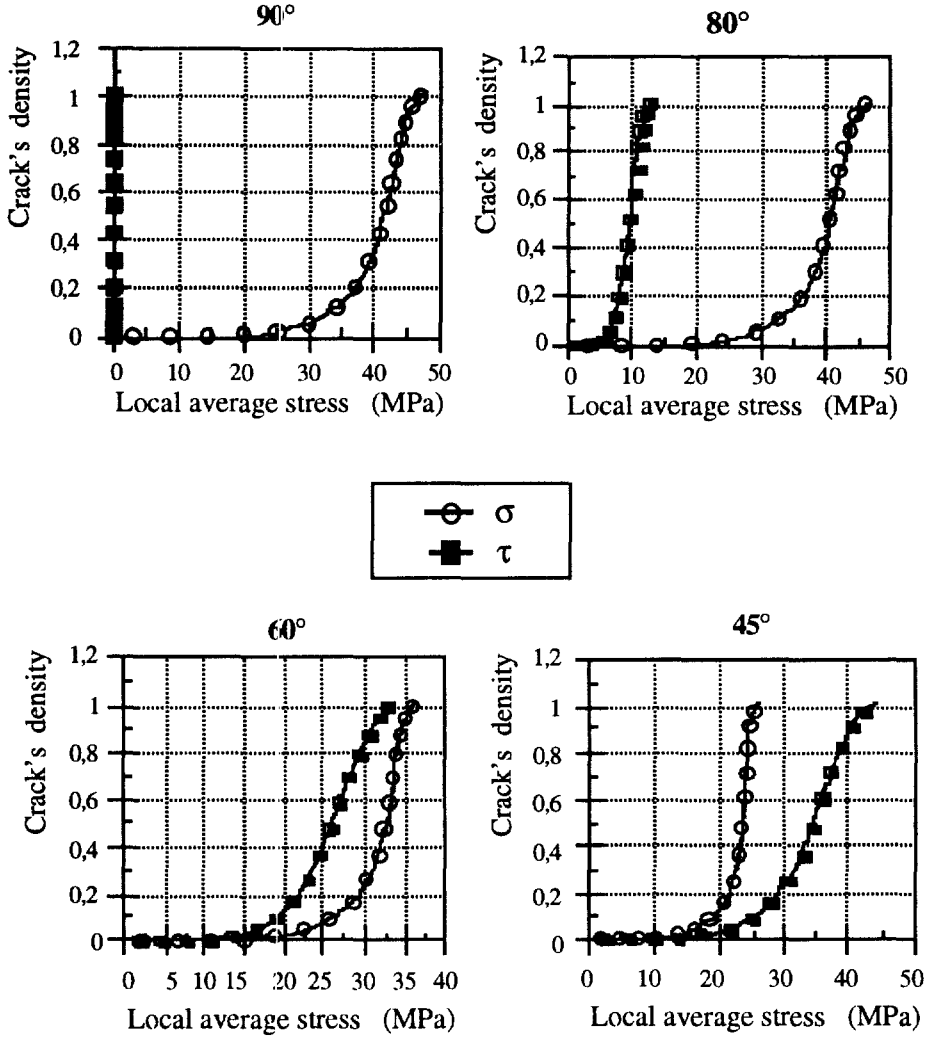

Fig. 13. Crack density as a function of the average stresses (σ, τ) calculated in the middle plies of the laminate (MPa).

All the curves shown on Fig. 13, present different average stress fields, as a function of the crack density: except for the flat laminate, a couple of stresses σ_{xx} and σ_{xy} is applied (from here now, one will use the notation σ and τ). The closer the angle α is to 45°, the higher is τ, as compared to σ.

6.2. *Fracture criterion for off axis tests and identification of the population of defects*

Angle ply laminates are submitted to a complex stress field in the middle plies and an important coupling relation exists between σ and τ. The following two assumptions are used in this work (α being the orientation of the stacking sequence and D the crack density).

- The local fracture criterion, combining the normal stress σ and the shear stress τ, is quadratic, as the macroscopic Tsai–Hill (Tsai, 1984) criterion used in composite materials (Petitpas, 1993):

$$\sigma^2(D,\alpha)+b^2\tau^2(D,\alpha)=f^2(D,\alpha). \tag{6}$$

It is assumed that the fracture of a SVE will take place when $f(d,\alpha) \geqslant f_c(D,\alpha)$, f_c being the critical (and random) value of the given SVE. The quadratic criterion depends on a coefficient b, enhancing the weakness of defects to shear.

- Whatever the defects that occur, their onsets are described by the law corresponding to the flat laminate $[0_2, 90_2]_s$. For this type of material, this leads to the expression:

$$f^2(D, 90) = \sigma_{eq}^2(D, 90) \tag{7}$$

where $\sigma_{eq}^2(D, 90)$ is the stress in the middle plies for the defect density D. With this assumption, we can use for identification the population of defects studied in section 4.3. The last parameter of the model is the coefficient b. All sequences of stacking are computed using values of $b = 0.5$, 1.0 and 1.4.

According to the second assumption, the loading induces only mode I fracture in the material. This is realistic because the shear stress τ results from shear efforts in a plane orthogonal to the crack lips. Therefore, one can consider that it cannot induce a mode II or III fracture; in addition, this assumption allows us to consider a part of the criterion as intrinsic to angle ply laminate and, consequently, to be able to make the corresponding identification from flat laminates.

6.3. *Prediction of the damage kinetics*

The method introduced previously for coupling the f.e. method with the fracture statistics is implemented in this section. Tridimensional meshes (up to 2500 f.e. with eight nodes and a quadratic interpolation) are used to study several aspects:

(i) assessing the validity of the quadratic criterion of fracture (is the coefficient b constant?);
(ii) study of the convergence of the f.e. problem;
(iii) study of the influence of the number of SVE on the results.

The first point is treated with the following choices of the coefficient, as mentioned earlier: $b = 0.5$, 1.0 and 1.4. From the results obtained for angle ply laminates ($\alpha = 80$, 60 and 45°, using 10 SVE), the calculated behavior is independent on b (Lebon, 1995). We decide, therefore, to choose from now on $b = 1.0$. For the second aspect, the same problem was solved with increasingly refined meshes and no significant change was observed in results.

The third aspects is very important because the adopted modeling induces an "all or nothing" behavior. That means that when the fracture stress is reached in one of the finite elements of a SVE, one immediately softens it by substituting a damaged one to its initial rigidity. In addition, increasing the number of SVE is equivalent to increasing the size of the specimen; from this, size effects on fracture can be studied.

To study the influence of the number of SVE, one calculates the behavior for different angle ply laminates ($\alpha = 80$, 60 and 45°) and for different number of SVE (10 and 50). Some results are given for $\alpha = 45°$ in Fig. 14, to compare with a damaged one (Fig. 12

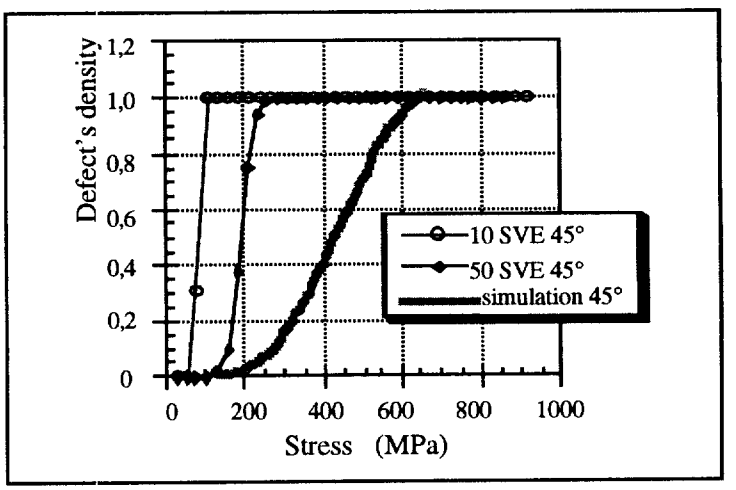

Fig. 14. Prediction of the damage kinetics for the off axis fracture of a laminate composite ($\alpha = 45°$).

obtained for $\alpha = 90°$). One notices that the more the laminate is off axis, the more the calculated results are different from the continuous damage approach. When $\alpha = 80$ and 90°, the results are very similar, whatever the number of SVE, and are close to the continuous approach. When $\alpha = 45$ and 60°, different results are obtained when changing the number of SVE: from this size effect, it appears that increasing the number of SVE gives results closer to the continuous model. Consequently, it is important for the off axis tests to define a minimum number of SVE to insure a good accuracy in the simulations.

7. CONCLUSION

The methodology developed for modeling the statistical aspects of fracture of laminate composites is successful for simple solicitations. Concerning the off axis fracture, the damage kinetics obtained from simulations is pessimistic, as compared to the results of a continuous numerical simulation. For large off axis laminates, it is necessary to perform experimental tests to evaluate the validity of our numerical simulations.

The main contribution of our approach is the use of models for the critical defects based on a large amount of data obtained by multi-fragmentation and multicracking tests, and introduced into finite element calculation by means of a statistical volume element. This approach is quite general, and can be applied to the simulation of the fracture of any material, where the length scale of the defects L_s and of a single unit of fracture L_d are provided (as the 0.5 and 0.1 mm scales in the present case for fibers). To improve the model, one can propose the following modifications:

- to introduce a continuous statistical damage model, in order to reduce the "all or nothing" effects of the behavior;
- to use more complex behavior laws for the plies. As one can see on experimental curves, laminates have nonlinear behavior (probably viscoelastic), that can be introduced in the modeling;
- to improve the implementation of the local "weakest link" hypothesis, by accounting for the heterogeneity of the stress field inside each SVE.

Acknowledgements—The authors wish to thank E. Munier, H. Burlet, P. Pilvin and G. Cailletaud of the Centre de Matériaux, Ecole des Mines de Paris, for their help in the computational part of this study. This research was supported by the CNES (Centre National des Etudes Spatiales, France) and DRET (Direction des Recherches et Etudes Techniques, France) under contracts 89/CNES3651 and 84/149.

REFERENCES

Bader, M. G. and Priest, A. M. (1982) Statistical aspects of fiber and bundle strength in hybrid composites. *Progress in Science and Engineering of Composites*, ed. T. Hayashi, K. Kawata and S. Umekawa, *Proceedings of ICCM-IV*, Tokyo, pp. 1129–1136.

Batdorf, S. B. (1982) Tensile strength of unidirectionaly reinforced composites—I. *Journal of Reinforced Plastics and Composites*, 1982, **1**, 153–164.

Baxevanakis, C., Jeulin, D. and Valentin, D. (1993a) Fracture statistics of single fiber specimens. *Composites Science and Technology* Vol. 48, 47–56.

Baxevanakis, C., Boussuge, M., Jeulin, D., Munier, E. and Renard, J. (1993b) Simulation of the development of fracture in composite materials with random defects. *MECAMAT 93, International Seminar on Micromechanics of Materials*, Eryrolles, Paris, pp 460–471.

Baxevanakis, C. (1994) Fracture statistics of laminates composites. Ph.D. thesis, Ecole Nationale Supérieure des Mines de Paris, December 1994.

Baxevanakis, C., Jeulin, D. and Renard, J. (1995) Fracture statistics of a unidirectional composite. *International Journal of Fracture* **73**, 149–181.

Burlet, H. and Cailletaud, G. (1986) Numerical Techniques for cyclic plasticity at variable temperature. *Engineering Computations* **3**, 143–154.

Hedgepeth, J. M. (1961) Stress concentrations in elementary structures. NASA TN D-882, Langley Research Center.

Jeulin, D. (1991) Modèles morphologiques de structures aléatoires et de changement d'echelle. Thèse d'Etat, Université de Caen.

Jeulin, D., Baxevanakis, C. and Renard, J. (1995) Statistical modelling of the fracture of laminate composites. *Applications of Statistics and Probability, Proceedings of the ICASP 7 Conference*, Paris, France, 1995, ed. M. Lemaire, J. L. Favre and A. Mebarki, Balkema.

Lebon, B. Study and modelisation of the damage of Sic/Sic woven composites. Ph.D. thesis, Ecole Nationale Supérieure des Mines de Paris, June 1993.

Lebon, B., Baxevanakis, C , Jeulin, D. and Renard, J. (1995) Fibers, composite materials, ceramics. Fracture statistical behavior of laminate composites. Final report DRET/ARMINES, ENSMP, Center of Materials P.M. Fourt, 1995.

Petitpas, E. (1993) Behavior and damage of stratified composite materials. Ph.D. thesis, Ecole Nationale Supérieure des Mines de Paris, June 1993.

Reifsnider, K. L. and Highsmith, A. L. (1982) Stiffness reduction mechanisms in composite laminates. *Damage in Composite Materials*, ASTM STP 775.

Renard, J. and Thionnet, A. (1993a) Meso macro approach to transverse cracking in composite laminated using Talreja's model. *Composites Engineering* **3**(9), 851–871.

Renard, J., Favre, J. P. and Jeggy, T. (1993b) Influence of transverse cracking on ply behavior: introduction of a characteristic damage variable. *Science Composites and Technology* **46,** 2937.

Sanchez Palencia, E. and Zaoui, A. (1987) *Homogenization Techniques for Composite Media.* Springer, Berlin.

Smith, R. S. and Phoenix, S. L. (1981) Asymptotic distributions for the failure of fibrous materials under series-parallel structure and equal load sharing. *Journal of Applied Mechanics* **48,** 48–75.

Tsai, S. W. (1984) A survey of macroscopic failure criteria for composite materials. *Journal of Reinforced Plastics and Composites* **3**(43), 40–62.

Wang, A. S. D. (1984) Fracture mechanisms of sublaminate cracks in composite materials. *Composites Technology Review* **6,** 45–62.

APPENDIX

Elements of homogenization

The homogenization method (Sanchez Palencia, 1987; Lebon, 1993) is obtained by averaging: let Ω be a domain of R^3 occupied by a heterogeneous body. Ω is related to the axis (x_i), and contains no defect (pores or cracks). The different inclusions are firmly bonded at the interface. Homogenization attempts to substitute a heterogeneous medium by an equivalent homogeneous one in which heterogeneities have been "rubbed out".

The main step of the method is the choice of a representative cell $V(y)$ (with the boundary ∂V) related to the axis (y_i). Two scales are present: a macroscopic one related to (x_i), in which heterogeneities are very small, and a microscopic one related to (y_i) (Fig. 6). A usual method for linking the two scales is to assume that macroscopic properties are the average of their corresponding microscopic properties.

Therefore, if (Σ, E) and (σ, ε) are, respectively, macroscopic and microscopic stress and strain tensors, we have the relations:

$$\Sigma_{ij} = \frac{1}{\text{mes}(V)} \int_V \sigma_{ij}(y)\,\mathrm{d}y = \langle \sigma_{ij} \rangle_V$$

$$E_{ij} = \frac{1}{\text{mes}(V)} \int_V \varepsilon_{ij}(y)\,\mathrm{d}y = \langle \varepsilon_{ij} \rangle_V. \tag{A1}$$

These relations have to be modified if the material contains defects such as cracks or pores. The problem P to solve is to find (σ, u), as the solution of:

$$\begin{aligned} \sigma_{ij,j} &= 0 \quad \text{in } V \\ \sigma_{ij} &= a_{ijkh}\varepsilon_{kh} \quad \text{in } V \\ \langle \varepsilon_{ij}(u) \rangle_V &= E_{ij} \quad \text{in } V + \text{boundary conditions on } \partial V. \end{aligned} \tag{A2}$$

We know that:

$$\Sigma_{ij} = \langle \sigma_{ij} \rangle_V = \langle a_{ijkh}\varepsilon_{kh} \rangle_V \tag{A3}$$

assuming that **D**, the strain localization tensor, is defined as $\varepsilon_{ij} = D_{ijkh}E_{kh}$, then

$$q^{\text{hom}}_{ijkh} = \langle a_{ijpq}D_{pqkh} \rangle_V \tag{A4}$$

where $\mathbf{q}^{\text{hom}}$ is the stiffness tensor of the equivalent homogeneous material associated with Ω. The accuracy of this method depends on the choice of **D**.

In the present case, an improvement of the Hill–Mandel approach was investigated: firstly the representative cell is chosen as the unit cell Y of a Y-periodic medium; then the periodicity of displacement is introduced. The problem P is now to find (σ, u) by solving:

$$\begin{aligned} \sigma_{ij,j} &= 0 \quad \text{in } V \\ \sigma_{ij} &= a_{ijkh}\varepsilon_{kh} \quad \text{in } V \\ u_i &= E_{ij}y_j + v_i \quad \text{on } \partial V \\ \text{with } v_i Y \text{ periodic if } E_{ij}y_j &= 0 \quad \text{and } v_i = 0 \quad \text{if } E_{ij}y_j \neq 0. \end{aligned} \tag{A5}$$

With these conditions, it can be proved that $\langle \varepsilon_{ij}(u) \rangle_V = E_{ij}$. The problem being linear in u, we can assume that

$$u_i = E_{kh} W_i^{kh}. \tag{A6}$$

The problem P is then split into six elementary problems (P^{kh}): find (s^{kh}, W^{kh}) solution of P for $k, h = 1, 2, 3$ and

$$E_{ij}^{kh} = \tfrac{1}{2}(\delta_{ik}\delta_{jh} + \delta_{ih}\delta_{jk}). \tag{A7}$$

Finally, we obtain the homogenized behavior from:

$$q_{ijkh}^{\text{hom}} = \langle s_{ij}^{kh} \rangle_V. \tag{A8}$$

This method is implemented to obtain the macroscopic behavior of laminates.